

Tunable charge carriers and thermoelectricity of single-crystal $\text{Ba}_8\text{Ga}_{16}\text{Sn}_{30}$

This article has been downloaded from IOPscience. Please scroll down to see the full text article.

2006 J. Phys.: Condens. Matter 18 1585

(<http://iopscience.iop.org/0953-8984/18/5/011>)

View [the table of contents for this issue](#), or go to the [journal homepage](#) for more

Download details:

IP Address: 129.252.86.83

The article was downloaded on 28/05/2010 at 08:53

Please note that [terms and conditions apply](#).

Tunable charge carriers and thermoelectricity of single-crystal $\text{Ba}_8\text{Ga}_{16}\text{Sn}_{30}$

M A Avila¹, D Huo^{1,2}, T Sakata¹, K Suekuni¹ and T Takabatake¹

¹ Department of Quantum Matter, ADSM, Hiroshima University, Higashi-Hiroshima 739-8530, Japan

² Department of Applied Physics, Hangzhou Dianzi University, Hangzhou 310018, People's Republic of China

Received 15 October 2005

Published 17 January 2006

Online at stacks.iop.org/JPhysCM/18/1585

Abstract

We have grown single crystals of the type-VIII intermetallic clathrate $\text{Ba}_8\text{Ga}_{16}\text{Sn}_{30}$ from both Sn and Ga fluxes, evaluated their compositions through electron microprobe analysis and studied their transport properties through measurements on the temperature dependent resistivity, thermopower and Hall coefficient. Crystals grown in Sn flux show n-type carriers and those from Ga flux show p-type carriers, whereas all measured compositions remain very close to the stoichiometric 8:16:30 proportion of Ba:Ga:Sn, expected from charge-balance principles. Our results indicate a very high sensitivity of the charge carrier nature and density with respect to the growth conditions, leading to relevant differences in transport properties which point to the importance of tuning this material for optimal thermoelectric performance.

(Some figures in this article are in colour only in the electronic version)

1. Introduction

Research on intermetallic clathrate compounds with general formula $\text{A}_8\text{X}'_{16}\text{X}_{30}$ ($\text{A} = \text{Ba}, \text{Sr}, \text{Eu}$; $\text{X}' = \text{Al}, \text{Ga}, \text{In}$; $\text{X} = \text{Si}, \text{Ge}, \text{Sn}$) has increased significantly over the past ten years, since the proposal that the generic class of caged compounds with guest atoms might be good candidates for realizing the phonon-glass electron-crystal (PGEC) concept of a thermoelectric material with potential for applications [1]. The cages in these clathrates are formed by $\text{X}'\text{X}$ host atoms connected through diamond-like hybridized orbitals, while the A guest atom lies within the cage and donates two electrons to it. For each divalent A ion in this particular family, the replacement of two X atoms with X' ions in the cage appears to be the required charge-balance condition for these two electrons to be accepted and for the structure to be stabilized.

The potential phonon-glass behaviour results from the fact that the A^{2+} ion can in certain cases be loosely bound inside a cage that is slightly oversized in comparison with its ionic

radius, and is thus able to achieve a rather independent ‘rattling’ motion that tends to scatter low frequency acoustic phonons, responsible for a good fraction of the heat conduction in a crystalline lattice [2]. In the case of $\text{Sr}_8\text{Ga}_{16}\text{Ge}_{30}$ and $\text{Eu}_8\text{Ga}_{16}\text{Ge}_{30}$, the additional presence of a fourfold splitting of an A atom site and the consequent tunnelling of this ion between these four off-centre sites is claimed to be the source of truly glass-like behaviour in their thermal conductivities at low temperatures [3–6]. The electron-crystal characteristic of these clathrates is preserved because the charge carriers remain within the cage network and are not significantly affected by the rattling motion of the guest atom.

We have recently reported a thorough characterization of the basic physical properties of the type-VIII clathrate $\text{Ba}_8\text{Ga}_{16}\text{Sn}_{30}$, grown as large single crystals out of Sn flux [7]. Electron probe microanalysis (EPMA) showed that these crystals grew with composition very close to 8:16:30 despite the excess Sn flux, confirming the relevance of the above-mentioned charge balance in the stabilization of the structure. These crystals showed behaviour consistent with a heavily doped n-type semiconductor with large negative thermopower and negative Hall coefficient. They also showed low lattice thermal conductivity of order $1 \text{ W m}^{-1} \text{ K}^{-1}$ resultant from the rattling of Ba ions, which was evidenced by large isotropic displacement parameters in single-crystal x-ray diffraction analysis and the presence of Einstein vibrational degrees of freedom in the heat capacity analysis.

Towards the end of the experimental investigations for that work, we also succeeded in growing single-crystalline $\text{Ba}_8\text{Ga}_{16}\text{Sn}_{30}$ out of Ga flux, and EPMA analysis once again showed a crystal composition very close to 8:16:30. Since these Ga flux crystals did not grow as easily or as large as the Sn flux ones, and the final composition was not significantly changed, they were not investigated in detail for that initial characterization. However, a recent study of sintered samples of $\text{Ba}_8\text{Ga}_{16+x}\text{Sn}_{30-x}$ (x being the *nominal* composition) showed that the carrier changes from electron type for $x \leq -2$ to hole type for $x \geq -1$ [8]. This result invited a more careful investigation on the dependence of our crystal’s properties on their growth conditions.

In the present work, we extend and complete the basic characterization of single-crystalline $\text{Ba}_8\text{Ga}_{16}\text{Sn}_{30}$ with a comparative study of Sn flux and Ga flux grown crystals. We will show that the transport properties are in fact highly sensitive to composition and/or growth conditions, and thus this material has a potential *tunability* that may in principle allow significant improvements in terms of its thermoelectric performance, in conjunction with other materials science techniques for this.

2. Experimental details

Four single-crystal batches were prepared and measured for this work: two using excess Sn flux and two using excess Ga flux. Samples from these batches will be referred to as Sn#1, Sn#2, Ga#1 and Ga#2 respectively. Sn#1 samples are from the same crystal growth as was described in detail in the previous work [7] using a Ba:Ga:Sn starting proportion of 8:16:60, and Sn#2 samples are from a second batch of crystals grown by essentially the same route. With Sn flux the crystals tend to grow very large (limited mostly by the total mass of the starting reagents and by the quartz tube size of order 10 mm in diameter) and have very well defined polyhedral surface facets.

For the Ga#1 and Ga#2 growths the starting elemental proportions were 8:26:30 and 8:50:30 respectively. The high purity elements were sealed in evacuated quartz tubes, soaked above 1150°C for 2–3 h, cooled over 10 h to 550°C and then slowly cooled over 100 h to 420°C . At this point the ampoules are quickly removed from the furnace and the remaining

Table 1. Relative Ba:Ga:Sn content in the four measured crystals as determined by electron probe microanalysis, and Fermi energies derived from thermopower analysis.

Batch name	Starting composition	Crystal composition			E_F (meV)
		Ba	Ga	Sn	
Sn#1	8:16:60	8	16.0	30.0	88
Sn#2	8:16:60	8	15.9	30.1	175
Ga#1	8:26:30	8	16.1	29.9	225
Ga#2	8:50:30	8	16.3	29.7	525

molten Ga flux separated by centrifuging. If the crystals did not grow to sufficient size in this first round, the solidified material was resealed with enough new Ga to complete the initial Ba:Ga:Sn proportion once again, and only the second part of the ramp was repeated. Polyhedral crystals grown from this approach were never larger than about 3 mm in diameter, and usually much smaller. Some of our growth attempts also resulted in large plate-like crystals rather than the expected polyhedra. EPMA analysis showed that these plates are a new compound BaGa_3Sn , which we intend to characterize and describe in a future communication.

To ensure the best possible reliability of a comparative EPMA evaluation of the Sn and Ga flux grown $\text{Ba}_8\text{Ga}_{16}\text{Sn}_{30}$ crystals, we mounted one crystal from each batch on a single sample holder and measured all four in a single experimental session at a JEOL JXA-8200 microanalyser, using the same reference materials for Ba, Ga and Sn. The results (averaged over five different regions for each crystal) are shown in table 1. All crystal compositions remain close to the nominal 8:16:30 proportion, but there are clear distinctions. Sample Sn#1 is, within experimental error, in the ideal stoichiometry. Samples Sn#2 and Ga#1 show an average slight excess of Sn and Ga respectively, and sample Ga#2 showed the greatest off-stoichiometry composition (excess Ga).

DC electrical resistivity experiments in the range of 4–300 K were performed on a home-made probe inserted into a glass cryostat. Crystals were shaped into elongated bars using a spark cutter and gold wire contacts were attached with silver paste, in standard four-probe geometry. For each point the average voltage was obtained from measurements with the current (1–10 mA) applied in opposite directions. Thermopower from 4–300 K was measured by a differential method, performed on a home-made probe inserted into a glass cryostat. The bar-shaped samples were suspended between two electrically isolated copper blocks, across which a temperature difference of 0.05–0.3 K was applied. The Hall coefficient from 4 to 300 K was measured on a home-made probe by a DC technique in a field of 1 T applied by a conduction magnet. Crystals were shaped into thin rectangular plates using a spark cutter and gold wire contacts were attached by spot welding.

3. Experimental results

The resistivity behaviour $\rho(T)$ below room temperature for all samples is shown in figure 1. They are in the $\text{m}\Omega \text{ cm}$ range and show monotonically decreasing values upon cooling, characteristic of heavily doped semiconductors or low carrier density metals. Since these are large, dense and carefully cut samples (rectangular cross-sections of order $A = 1 \text{ mm}^2$) the uncertainty in estimating the geometrical factor A/d is relatively small ($<5\%$), so the differences observed in the calculated resistivities should not be resultant from trivial geometrical uncertainty. The quasi-stoichiometric Sn#1 sample has the highest resistivity,

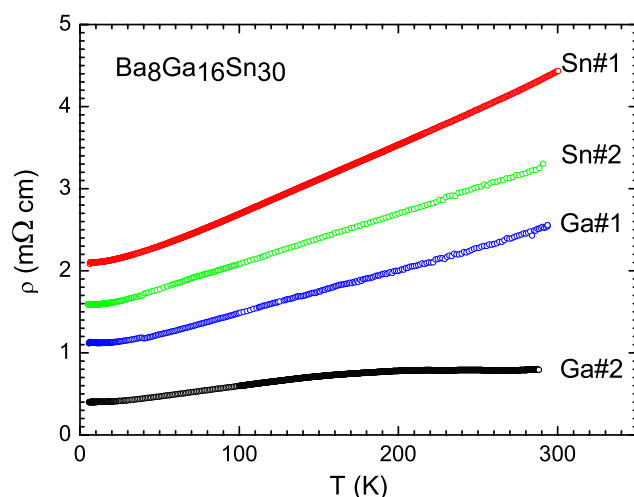


Figure 1. Temperature dependence of the electrical resistivity $\rho(T)$ of $\text{Ba}_8\text{Ga}_{16}\text{Sn}_{30}$ crystals grown from Sn and Ga flux.

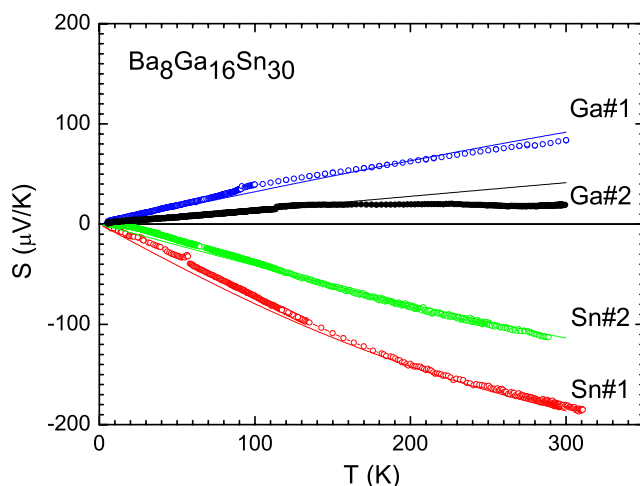


Figure 2. Temperature dependence of the thermoelectric power $S(T)$ of $\text{Ba}_8\text{Ga}_{16}\text{Sn}_{30}$ crystals grown from Sn and Ga flux. Solid lines are the best fits of a single-band model.

consistent with the idea that the ideal material tends towards a narrow gap semiconductor. But none of the $\text{Ba}_8\text{Ga}_{16}\text{Sn}_{30}$ crystals grown so far have shown semiconducting resistivity like that of $\text{Ba}_8\text{Ga}_{16}\text{Ge}_{30}$ [9], so the question remains open whether there is a true gap or a pseudo-gap in the ideal material. The Sn#2 and Ga#1 samples have smaller resistivities, as one would expect from the electron and hole doping effect of their respective off-stoichiometries, and the Ga#2 sample has the lowest resistivity, consistent with its largest doping level.

The differences between the charge carrier types and their densities become much more evident in the thermopower measurements. In figure 2 we show $S(T)$ for the same samples in figure 1. As shown in the previous work, Sn#1 sample has negative, monotonically decreasing thermopower over the entire temperature interval (n-type carriers) and reaches a relatively

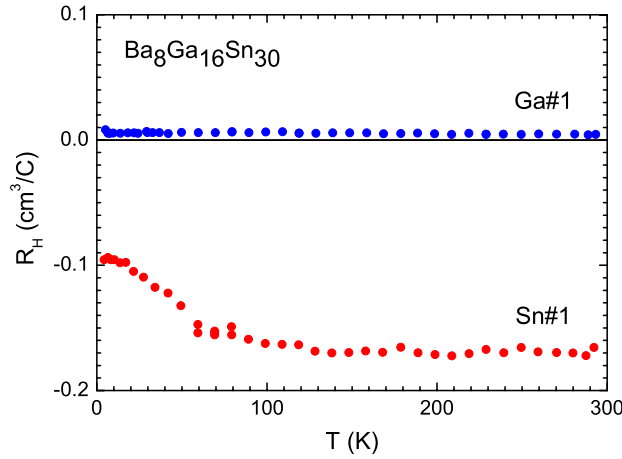


Figure 3. Temperature dependence of the Hall coefficient R_H of $\text{Ba}_8\text{Ga}_{16}\text{Sn}_{30}$ crystals grown from Sn and Ga flux.

large magnitude of $-185 \mu\text{V K}^{-1}$ at 290 K. The Sn#2 sample shows somewhat smaller but qualitatively similar behaviour, reaching $-113 \mu\text{V K}^{-1}$ at 290 K. In contrast, the two Ga flux samples show positive $S(T)$ over the entire measured interval, indicating p-type carriers. Sample Ga#1 reaches $+83 \mu\text{V K}^{-1}$ at 290 K, while sample Ga#1 remains below $+20 \mu\text{V K}^{-1}$. The solid lines show the best fits of these $S(T)$ curves to the equation

$$S(T) = \frac{k_B}{e} \left(\frac{4F_3(E_F/k_B T)}{3F_2(E_F/k_B T)} - E_F/k_B T \right) \quad (1)$$

derived for a single-parabolic-band model [10], where F_n is the Fermi–Dirac integral of order n , and the only fitting parameter is the Fermi energy E_F , whose respective values are listed in table 1. It is reasonable to assume that this system should be better described by a two-band model though.

Further confirmation of these distinctions for different fluxes came with the Hall coefficient measurements, shown in figure 3. A sample from batch Sn#1 shows negative R_H over the entire temperature interval, while a sample from batch Ga#1 showed a very small and positive R_H . From the single-band model [10], the carrier concentrations $n = 1/eR_H$ obtained from these measurements at 300 K are 3.7×10^{19} electrons cm^{-3} and 1.3×10^{21} holes cm^{-3} respectively. The temperature dependence of the Hall mobility $\mu_H(T) = |R_H(T)|/\rho(T)$ derived from these measurements is plotted in figure 4. The respective values at 290 K are 39 and $1.8 \text{ cm}^2 \text{ V}^{-1} \text{ s}^{-1}$, and for both samples a negative slope is seen at higher temperatures, approaching a $T^{-3/2}$ law expected from acoustic phonon scattering [11], indicating that this should be the dominant scattering mechanism in this region.

4. Discussion

The principle of operation of a thermoelectric cooling device requires a pair of materials, one of n type and one of p type, coupled electrically in series and thermally in parallel [12]. The device's performance optimization involves not only the properties of each individual branch, but also a combined optimization of the thermoelectric pair. Thus, an important goal of research in this area is to not only find good thermoelectric materials of both carrier types, but also find

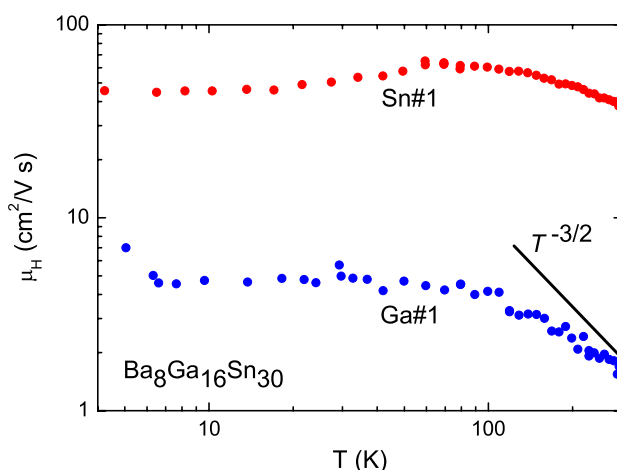


Figure 4. Temperature dependence of the Hall mobility μ_H of $\text{Ba}_8\text{Ga}_{16}\text{Sn}_{30}$ crystals grown from Sn and Ga flux.

materials that may be fine-tuned with respect to their figure of merit $ZT = S^2T/\rho\kappa$. Our experiments show that $\text{Ba}_8\text{Ga}_{16}\text{Sn}_{30}$ samples may be candidates for fulfilling most of these requirements, if its present ZT of order 0.15 at room temperature [7] can be improved to closer to unity.

The existence of n-type and p-type samples has already been observed in sintered samples with nominal compositions $\text{Ba}_8\text{Ga}_{16+x}\text{Sn}_{30-x}$ [8]. It was reported that a gradual decrease of n-type carriers for $-3 < x < -2$ is followed by a gradual increase of p-type carriers for $-1 < x < +2$, with a possible ‘quasi-insulating’ region around $x = -1.5$. Our results clearly show that the flux grown crystals are strikingly more sensitive in terms of sample composition, such that off-stoichiometries of $x = \pm 0.1$ from the ideal value are enough to cause the drastic change. This also raises the question of whether the substantially deviated *nominal* compositions assumed for the polycrystals truly reflect their actual intra-grain clathrate compositions.

If we can understand the reasons behind the observed differences in carriers and transport properties, we may be able to control these through the growth parameters and/or through post-growth thermal treatment. The first issue is whether the observed differences are indeed primarily associated with off-stoichiometry. Our experimental data give good evidence that there is in fact a correlation with the Ga–Sn proportion, such that the transport properties can be directly related to the ionic self-doping level.

But the transport properties may not be directly related only to differences in composition. The next logical step is to account for differences in the distribution of Ga–Sn atoms throughout the cage structure. Unlike in the Ga–Ge clathrates where, due to size similarity of these two atoms, a mostly random distribution is shown throughout all three crystallographic sites of the type-I clathrate structure (although there are some indications of possible preferential occupations) [4, 13, 14], in $\text{Ba}_8\text{Ga}_{16}\text{Sn}_{30}$ the size difference between Ga and Sn ions is large enough that there is a clear preferential occupation of at least three of their four different sites in the type-VIII clathrate structure. Assuming that random occupation of a given site implies a proportion close to $\text{Ga}_{16}\text{Sn}_{30}$ in that site, the single-crystal XRD refinement on the Sn#2 crystal performed for the previous work [7] revealed that Sn tends to favour the X(1) site ($\text{Ga}_{8.5}\text{Sn}_{37.5}$) and X(2) site ($\text{Ga}_{7.3}\text{Sn}_{38.7}$) while Ga tends to occupy the X(4) site ($\text{Ga}_{35.3}\text{Sn}_{10.7}$) which has

the shortest bond distances between neighbours, and the X(3) site remains more randomly occupied by both atoms ($\text{Ga}_{14.4}\text{Sn}_{31.6}$). We performed a preliminary comparative investigation of the Sn#2 crystal before and after annealing for one week at 480 °C, which showed only a 12% decrease in its thermopower above room temperature, so that either the annealing condition was ineffective in significantly rearranging the as grown Ga–Sn distribution or the differences in distribution may be indeed secondary with respect to thermoelectric properties, in comparison to composition differences.

5. Conclusion

Single crystals of $\text{Ba}_8\text{Ga}_{16}\text{Sn}_{30}$ grown from Sn flux and Ga flux have shown significantly different charge carrier densities and transport properties, which we were able to correlate with the relative Ga–Sn content in the crystals. The crossover between n-type and p-type carriers occurs within a very narrow range around the ideal 8:16:30 stoichiometry, in agreement with charge-balance principles and contrary to previously reported preliminary studies on sintered polycrystals. Such characteristics point to the possibility of tuning the charge carrier nature and density, as well as the transport properties, through the sample preparation process and possibly through post-growth annealings, a desirable feature in any material intended for thermoelectric applications. Our next step is now to investigate the low temperature heat capacity/conductance behaviour of the carrier-tuned $\text{Ba}_8\text{Ga}_{16}\text{Sn}_{30}$ crystals, in search of further information on the vibrational behaviour of the Ba guests ions under different host cage environments.

To our satisfaction, at almost the same time as we first submitted this manuscript, a research group from Dresden published two excellent works [15, 16] describing how their polycrystalline $\text{Eu}_8\text{Ga}_{16}\text{Ge}_{30}$ samples can be tuned with respect to composition, carrier concentration and thermoelectric properties, although in their case only n-type samples were found. Their results also challenge the current ‘tunnelling’ models for glass-like thermal conductivity (which we mentioned in the introduction section) attributing this low temperature behaviour to phonon–charge carrier scattering instead.

Acknowledgments

We thank Y Shibata for the electron probe microanalysis. This work was financially supported by the COE Research (CE13CE2002) and the priority area ‘Skutterudite’ (No 15072205) through Grants-in-Aid from MEXT, Japan. D Huo is also supported by the National Science Foundation of China (No. 50471008).

References

- [1] Slack G A 1995 *CRC Handbook of Thermoelectrics* (Boca Raton, FL: Chemical Rubber Company) chapter 34 p 407
- [2] Cohn J L, Nolas G S, Fessatidis V, Metcalf T H and Slack G A 1999 *Phys. Rev. Lett.* **82** 799
- [3] Sales B C, Chakoumakos B C, Jin R, Thompson J R and Mandrus D 2001 *Phys. Rev. B* **63** 245113
- [4] Chakoumakos B C, Sales B C and Mandrus D G 2001 *J. Alloys Compounds* **322** 127
- [5] Keppens V, McGuire M A, Teklu A, Laermans C, Sales B C, Mandrus D and Chakoumakos B C 2002 *Physica B* **316/317** 95
- [6] Zerec I, Keppens V, McGuire M A, Mandrus D, Sales B C and Thalmeier P 2004 *Phys. Rev. Lett.* **92** 185502
- [7] Huo D, Sakata T, Sasakawa T, Avila M A, Tsubota M, Iga F, Fukuoka H, Yamanaka S, Aoyagi S and Takabatake T 2005 *Phys. Rev. B* **71** 075113
- [8] Kurinaga T, Nagamoto Y, Ido S, Hayase H and Koyanagi T 2000 *Thermoelectric Conversion Symp. 2000 Proc. (Tokyo, Japan)* pp 84–5

-
- [9] Umeo K, Avila M A, Sakata T, Suekuni K and Takabatake T 2005 *J. Phys. Soc. Japan* **74** 2145
 - [10] Lovett D R 1977 *Semimetals and Narrow-BandGap Semiconductors* (London: Pion Limited)
 - [11] Seeger K 1985 *Semiconductors Physics: an Introduction* (New York: Springer)
 - [12] Nolas G S, Sharp J and Goldsmid H J 2001 *Thermoelectrics—Basic Principles and New Materials Developments* (New York: Springer)
 - [13] Chakoumakos B C, Sales B C, Mandrus D G and Nolas G S 2000 *J. Alloys Compounds* **296** 80
 - [14] Zhang Y, Lee P L, Nolas G S and Wilkinson A P 2002 *Appl. Phys. Lett.* **80** 2931
 - [15] Pacheco V, Bontien A, Carrillo-Cabrera W, Paschen S, Steglich F and Grin Y 2005 *Phys. Rev. B* **71** 165205
 - [16] Bontien A, Pacheco V, Paschen S, Grin Y and Steglich F 2005 *Phys. Rev. B* **71** 165206